



A NOVEL MODEL OF OPTIMALHYBRID CONTROL IN A SPACE VECTOR MODULATION SVM FOR VOLTAGE SOURCE INVERTER CONTROL

Juan Gabriel Jiménez Perdomo¹, Carlos Andrés Cuellar Perdomo², Carlos Alberto Pérez Camacho³ and Ruthber Rodríguez Serrezuela⁴

¹Faculty of Business Administration, Corporación Universitaria Minuto de Dios, Neiva, Colombia

²Mechanical Engineering, Universidad Antonio Nariño, Neiva, Colombia

³Manager of Electronics and Telecommunications, Servicio Nacional de Aprendizaje, Tecnoparque Neiva, Colombia

⁴Industrial Engineering Program, Corporación Universitaria del Huila, Neiva, Colombia

E-Mail: ruthbrodriguez@corhuila.edu.co

ABSTRACT

In our paper, we investigate the problem of optimal hybrid control for space vector modulation (SVM), applying a new optimal hybrid control approach for pulse width modulation (PWM). It is used for the creation of alternating current (AC) waveforms, which would be applied to three-phase motors using class D amplifiers. Our contribution demonstrates a reduction of the total harmonic distortion (THD) created by the rapid change inherent in the implementation of our algorithm. The results can be observed in the simulations obtained through the Matlab/Simulink software.

Keywords: hybrid control, space vector, labview, modulation.

INTRODUCTION

In the last decade, the use of optimal hybrid control in the solution of engineering problems in non-linear systems has taken on great importance (see e.g., [1], [2], [3]). For the control of Pulse Width Modulation (PWM) the algorithms of Space Vector Modulation (SVM) [4] is used, it is used for the generation of Alternating Current (AC) waveforms [5], [6], which allows to govern the dynamic behavior of three-phase AC motors [7].

There are variations of SVM that result in different quality and computational requirements. For the optimal hybrid control problem the main tool is the generation of optimal trajectories using the Maximum Hybrid principle, which is the generalized product of the maximum principle of Pontryagin classic [8], [9], [10].

Consequently, a variation of the Maximum Hybrid Principle for our Space Vector Modulation can be tested under the assumption of certain restrictive. In this way, these assumptions will ensure that classic "needle variations" will still be acceptable variations [13], [14], [15].

Based on the evolution of microprocessor performance, the demand for better performances in the drives and the generalization of the Park (1929) [16] and Clarke (1958) [17] transformations for the analysis of three-phase circuits. Van Der Broeck (1988) [18] achieved implement the PWM technique based on space vectors SV-PWM (Space Vector - PWM) that had already been proposed by Pfaff (1984) [19]. Currently, SV-PWM modulation has become a popular technique for three-phase inverters, particularly in induction motor control applications.

The reference space vector in the PWM modulation based on space vectors, the interaction between the three phases is exploited and instead of using a modulator for each phase, a single modulator is

processed for the space vector of voltage of the three-phase set [20], [21], [22].

There are variations of SVM that result in different quality and computational requirements [23], [24]. One active area of development is in the reduction of total harmonic distortion (THD) created by the rapid switching inherent to these algorithms [25], [26], [27].

Our paper is organized in the following way. In section 2, we find the problem of the formulation of optimal hybrid control, the methodology, the materials and some basic aspects. Session 3 is dedicated to showing the results and discussing the evaluation obtained from the optimal hybrid control problem used for the development of Space Vector Modulation (SVM). In section 4, we present the conclusions obtained from the computational approach used based on gradient for the initial problem of Space Vector Modulation (SVM) [28], [29], [30].

PROBLEM FORMULATION OPTIMAL CONTROL CLASSIC

The following linear equation represents a typical dynamic system:

$$\begin{cases} \dot{x}(t) = f(t, x(t), u(t)), & t \in [t_0, t_f] \\ x(t_0) = x_0 \end{cases} \quad (1)$$

In that: $f: [t_0, t_f] \times \mathbb{R}^n \times \mathbb{R}^m \rightarrow \mathbb{R}^n$. Mapping $u(\cdot): [t_0, t_f] \rightarrow \mathbb{R}^m$ better called control where $x_0 \in \mathbb{R}^n$ is the main part and the answer of (1) is a function continuous $x(\cdot): [t_0, t_f] \rightarrow \mathbb{R}^n$ called path state control $u(\cdot)$ [13], [14].

We must assume that for any x_0 and any controls $u(\cdot)$ there is one answer to the equation (1). In the same way, the control performance applied to the system is also calculated in the following way:



$$J(u(\cdot)) = \int_{t_0}^{t_f} g(t, x(t), u(t)) dt + h(x(t_f)) \quad (2)$$

Where $g : [t_0, t_f] \times \mathbb{R}^n \times \mathbb{R}^m \rightarrow \mathbb{R}$, $h : \mathbb{R}^n \rightarrow \mathbb{R}$ the term of the right member of the equation is called "running cost" and the left member of the equation is called "cost terminal". Normally we can find optimal control restrictions in the states of the system and in the control, these can be determined in the following way:

$$x(t) \in S, u(t) \in U, \forall t \in [t_0, t_f].$$

Where $S \subseteq \mathbb{R}^n$, $U \subseteq \mathbb{R}^m$. $u(\cdot)$ Or control is called admissible control, and the pair $(x(\cdot), u(\cdot))$ admissible if:

- a) $u(\cdot) \in U$.
- b) $x(\cdot)$ is the only continuous solution (1).
- c) the restriction status is satisfied.
- d) $t \rightarrow f(t, x(t), u(t)) \in L_1 [t_0, t_f]$.

The group of admissible controls is framed by $U_{adm} [t_0, t_f]$.

PONTRYAGIN'S PRINCIPLE OF MAXIMUM

In the theory of optimal control, the Maximum principle is very important. He states that any optimal control along with his state trajectory must fulfill the condition called the Hamiltonian system.

Also from the mathematical preamble of the maximum principle, it is easy to maximize the Hamiltonian system as the main argument.

Maximum principle: let $x^*(\cdot), u^*(\cdot)$. An optimal pair of classical optimal control, then there is a continuous function $p(\cdot) : [t_0, t_f] \rightarrow \mathbb{R}^n$

$$\begin{cases} \dot{p}(t) = f_t(x^*(t), u^*(t))^T p(t) + g_x(t, x^*(t), u^*(t)), \\ \quad t \in [t_0, t_f] \\ p(t_f) = -h_f(x^*(t_f)) \end{cases} \quad (3)$$

Where x is the partial derivative, o be;

$$f_x = \frac{\partial f}{\partial x}, \quad g_x = \frac{\partial g}{\partial x}, \quad h_x = \frac{\partial h}{\partial x}$$

$$H(t, x^*(t), u^*(t), p(t)) = \max_{u \in U}$$

$$H(t, x^*(t), u, p(t)), \quad t \in [t_0, t_f].$$

Where U represents the set of admissible controls plus:

$$H(t, x, u, p) = \langle p, f(t, x, u) \rangle - g(t, x, u), \quad (t, x, u, p) \in [t_0, t_f] \times \mathbb{R}^n \times U \times \mathbb{R}^n.$$

With $\langle \cdot, \cdot \rangle$ Represents the standard domestic product in \mathbb{R}^n .

THE HAMILTON-JACOBI-BELLMAN EQUATION AND DYNAMIC PROGRAMMING SYSTEM

We establish a dynamic system expressed as follows:

$$\begin{cases} \dot{x}(t) = f(t, x(t), u(t)), \\ x(t_0) = x_0 \end{cases} \quad t \in [t_0, t_f] \quad (4)$$

It is required to minimize the performance control supplied to the given system:

$$J(u(\cdot)) = \int_{t_0}^{t_f} g(x(t), u(t), t) dt + h(x(t_f)) \quad (5)$$

We must bear in mind that the initial conditions remain static [18], which is the initial time t_0 and the initial state $x(t_0) = x_0$.

A. MINIMUM TIME SWITCHED CONTROL

The problem of minimum time control is presented as a case of application for the Maximum Principle, in which a problem of optimization with restrictions is proposed, as follows:

$$J(u(\cdot)) = \int_{t_0}^{t_f} 1 dt = t_f - t_0$$

Subjected to $-1 \leq u(t) \leq 1$ and desired null end conditions for the vector of states (i.e. $\Psi(x(t_f)) = 0$), starting from arbitrary initial conditions [19]. Thus, the form taken by the Lagrangian system:

$$L(x, u) = 1$$

Where it is possible to formulate the corresponding Hamiltonian:

$$H(t, x^*(t), u, \lambda(t)) = 1 + \lambda^T f(x, u)$$

That for the case of a linear system:

$$\dot{x} = Ax(t) + B u(t)$$

By the principle of maximum, in an optimal solution of type [20]:

$$u(t) = -\text{sign}(B^T \lambda(t))$$

B. OPTIMAL HYBRID CONTROL OF SPACE VECTOR MODULATION

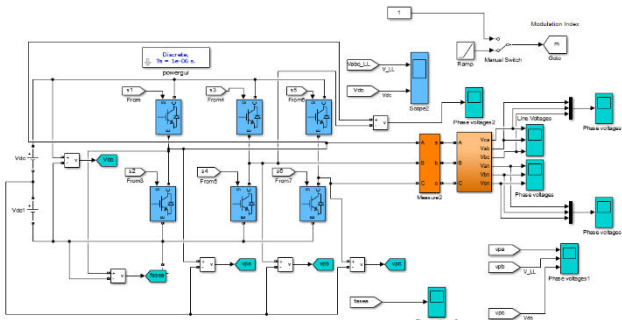


Figure-1. Three-phase inverter implemented in Matlab/ Simulink.

Space Vector Modulation relates to a special switching process that is based on the top switches of a three-phase matrix converter. Said switching can be carried out by using an optimal hybrid controller that adequately governs the phases of the inverter.

In the theory, SVM works a sinusoidal voltage as a phasor or amplitude vector that rotates at a constant angular frequency, ω . Said vector of constant amplitude is represented in the plane d-q where it means the real and imaginary axes respectively.

Because SVM takes the three signals or the modulation voltages as if they were a single unit, the vector sum of the three signals or the three modulating voltages are referred to as the reference voltage, V_{ref} . This magnitude is linked to the magnitude of the output voltage of the switching topologies.

The objective of the optimal hybrid control of the SVM is to approximate the reference voltage vector, V_{oref} of the switching topologies. If we have a three-phase network in equilibrium, the instantaneous voltages can be expressed as:

$$\begin{bmatrix} v_1(t) \\ v_2(t) \\ v_3(t) \end{bmatrix} = v_o \begin{bmatrix} \cos \omega_o t \\ \cos (\omega_o t - 120) \\ \cos (\omega_o t - 240) \end{bmatrix} \quad (6)$$

The above expression can be represented in terms of the complex spatial vector, thus:

$$\vec{V}_o = \frac{2}{3} \left[v_1(t) + v_2(t)e^{\frac{j2\pi}{3}} + v_3(t)e^{\frac{j4\pi}{3}} \right] = v_o e^{j\omega_o t} \quad (7)$$

For the property of Euler, we have:

$$e^{j\theta} = \cos \theta + j \sin \theta$$

Represents a phase shift operator and $\frac{2}{3}$ is a scaling factor equal to the ratio between the magnitude of the output line-to-line voltage and that of output voltage vector. The angular velocity of the vector is ω_o and its magnitude V_o .

Likewise, the representation of the spatial vector of the input voltage to the three-phase inverter will be given by:

$$\begin{bmatrix} v_a(t) \\ v_b(t) \\ v_c(t) \end{bmatrix} = v_i \begin{bmatrix} \cos \omega_o t \\ \cos (\omega_o t - 120) \\ \cos (\omega_o t - 240) \end{bmatrix} \quad (8)$$

$$\vec{V}_i = \frac{2}{3} \left[v_a(t) + v_b(t)e^{\frac{j2\pi}{3}} + v_c(t)e^{\frac{j4\pi}{3}} \right] = v_i e^{j\omega_o t} \quad (9)$$

Where the angular velocity of the vector is ω_i and its magnitude V_i . By connecting a balanced three-phase load to the inverter terminals, the equations of the spatial vector of the three-phase output and the input currents can be expressed as follows:

$$\begin{bmatrix} i_1(t) \\ i_2(t) \\ i_3(t) \end{bmatrix} = i_o \begin{bmatrix} \cos \omega_o t \\ \cos (\omega_o t - 120) \\ \cos (\omega_o t - 240) \end{bmatrix} \quad (10)$$

The above expression can be represented in terms of the complex spatial vector, thus:

$$\vec{I}_o = \frac{2}{3} \left[i_1(t) + i_2(t)e^{\frac{j2\pi}{3}} + i_3(t)e^{\frac{j4\pi}{3}} \right] = i_o e^{j(\omega_o t + \theta_o)} \quad (11)$$

Likewise, the representation of the spatial vector of the input currents to the three-phase inverter will be given by:

$$\begin{bmatrix} i_a(t) \\ i_b(t) \\ i_c(t) \end{bmatrix} = i_i \begin{bmatrix} \cos \omega_o t \\ \cos (\omega_o t - 120) \\ \cos (\omega_o t - 240) \end{bmatrix} \quad (7)$$

$$\vec{i}_i = \frac{2}{3} \left[i_a(t) + i_b(t)e^{\frac{j2\pi}{3}} + i_c(t)e^{\frac{j4\pi}{3}} \right] = i_i e^{j(\omega_o t + \theta_i)} \quad (12)$$

The equations of the three-phase inverter system present non-linearities of quadratic order and the currents present in the system have a linear behaviour to the square root of each of the phases. For the process of linearized equations of the three-phase inverter Taylor series are used and these are used to design a state feedback controller.

$$f_v = (x, u) = f_v(x_r, u_r) + \frac{\partial f}{\partial x} |_{x_r, u_r} (x - x_r) + \frac{\partial f}{\partial u} |_{x_r, u_r} (u - u_r) \quad (13)$$

Being $x \in R^{n \times 1}$ the state vector, u is the input signal to the robotic arm; x_r and u_r are the equilibrium points, then to find and evaluate the partial derivative $f(x_r, u_r)$ at breakeven, it is $f(0, 0)$:

$$\frac{\partial f}{\partial x} |_{(0,0)} = \begin{bmatrix} \frac{\partial f_1}{\partial x_1} & \frac{\partial f_1}{\partial x_2} & \frac{\partial f_1}{\partial x_3} \\ \frac{\partial f_2}{\partial x_1} & \frac{\partial f_2}{\partial x_2} & \frac{\partial f_2}{\partial x_3} \\ \frac{\partial f_3}{\partial x_1} & \frac{\partial f_3}{\partial x_2} & \frac{\partial f_3}{\partial x_3} \end{bmatrix}$$



$$\frac{\partial f}{\partial u} |_{(0,0)} = \begin{bmatrix} \frac{\partial f_1}{\partial u} \\ \frac{\partial f_2}{\partial u} \\ \frac{\partial f_3}{\partial u} \end{bmatrix}$$

The linearized state space model in continuous form is given in Equation:

Above

$$\dot{x}_i(t) = Ax(t) + Bu(t)$$

$$\begin{bmatrix} \dot{x}_1 \\ \dot{x}_2 \\ \dot{x}_3 \end{bmatrix} = \begin{bmatrix} \frac{\partial v_1}{\partial x_1} & 0 & 0 \\ 0 & \frac{\partial v_2}{\partial x_2} & 0 \\ 0 & 0 & \frac{\partial v_3}{\partial x_3} \end{bmatrix} \begin{bmatrix} x_1 \\ x_2 \\ x_3 \end{bmatrix} + \begin{bmatrix} \frac{1}{s} & 0 \\ 0 & 0 \\ 0 & \frac{1}{s} \end{bmatrix} u(t)$$

The developed matrices are described above in the continuous space, to be implemented in our system:

$$x_{k+1} = G x_k + K u_k \text{ 0.25 seconds.}$$

The goal is to calculate a permissible control law, which allows minimizing the value of the costs of the second functional level of the three-phase inverter.

$$J(u(\cdot)) = \frac{1}{2} \int_{t_0}^{t_f} [X^T(t) + QX(t) + u^T(t) + Ru(t)] dt \rightarrow \min_{u(\cdot)} \quad (14)$$

The resulting Linear Quadratic Regulator has the following form

$$u^{opt}(t) = -R^{-1}(t)B^T(t)P(t)X^{opt}(t) \quad (15)$$

where P (t) is a solution of the Riccati equation:

$$P(t) = -(A^T P(t) + P(t)A(t) + \dot{P}(t)B(t)R^{-1}(t)B^T(t)P(t) - Q(t)) \quad (16)$$

With the final condition:

$$P(t_f) = 0 \quad (17)$$

RESULTS

With the data obtained by modeling the three-phase inverter system, the system matrices were obtained in state variables and analyzed in the toolbox for Hybrid Systems of Matlab [15], [16].

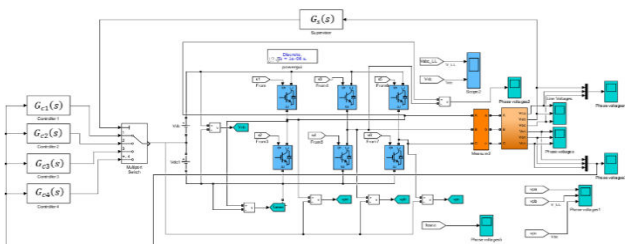


Figure-2. Block diagram of the hybrid control system developed in Simulink.

The first thing we do is perform an analysis of the frequency spectrum of the three-phase inverter to know what harmonics were being produced. As we can see in the graph, there is a harmonic content at 35 Hz, in the same way it can be seen that at 2.5 kHz a large content appears and between 4.5 KHz and 4.8 KHz. They are frequencies multiples of the fundamental working frequency of the system and whose amplitude decreases as the multiple increases, as we can see. These effects can be reduced by applying a filter to the inverter output.

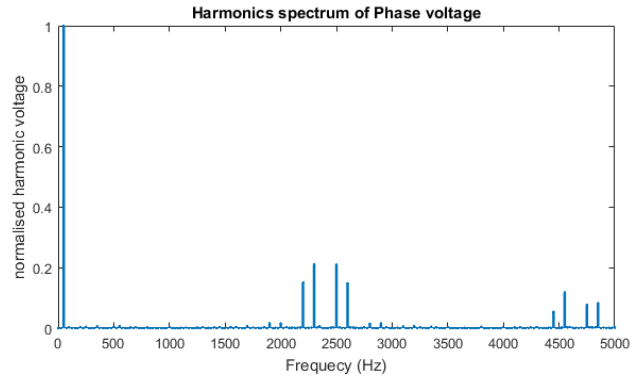


Figure-3. Harmonic spectrum of phase voltage.

As illustrated in Figure-4, the active vectors divide the ab plane into six sectors, forming the axes of a hexagon. This hexagon is known as the investor's hexagon. It shows the path of the spatial vector during the application of the optimal hybrid control [17], [18].

The angular frequency and the amplitude of the modulating signals respectively determine the rotation speed and the amplitude of the reference vector.

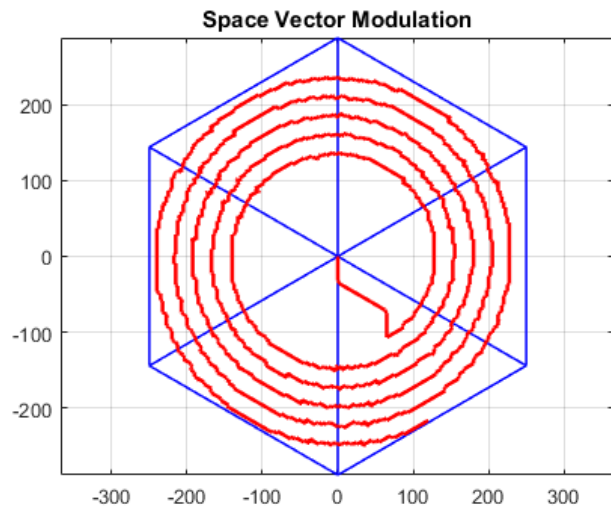


Figure-4. Space vector modulation.

There is the possibility of developing infinite modulation algorithms, given that theoretically an infinite number of zero sequence signals can be established. In a similar way, because the restrictions of performance and



implementation of the investors can be reduced to a very small number [19], [20].

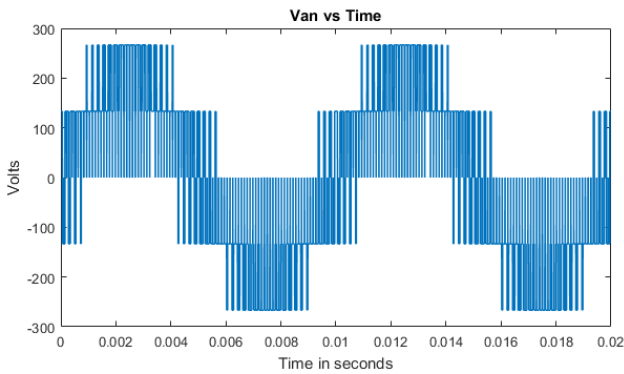


Figure-5. Voltage in one of the phases, Van.

In the Figures 6 and 7, we can observe the behaviour of each of the phases through the Space Vector Modulation [21], [22]. We can appreciate that the voltage for each phase is 220vpp, showing a THD = 0.8, which is a permissible value.

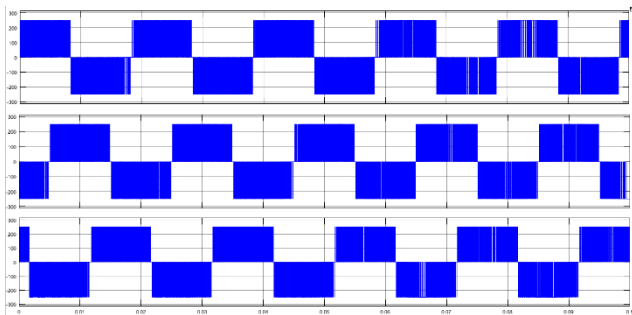


Figure-6. Voltage in three of the phases, Van, Vbn and Vcn.

The angle is generated from the reference output frequency by integrating it. Based on the angle, the sector can be identified [23], [24]. The result is shown in Figure-7.

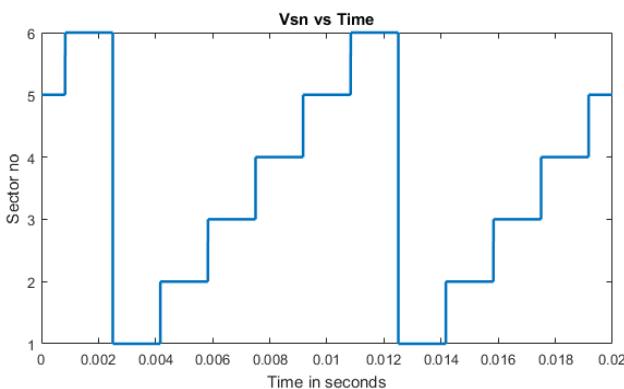


Figure-7. Duty ratio profile with standard SVPWM.

Carrier based SVPWM allow fast and efficient implementation of SVPWM without sector

determination. The technique is based on the duty ratio profiles that SVPWM exhibits (as shown in Figure-8). By comparing the duty ratio profile with a higher frequency triangular carrier the pulses can be generated, based on the same arguments as the sinusoidal pulse width modulation [25], [26].

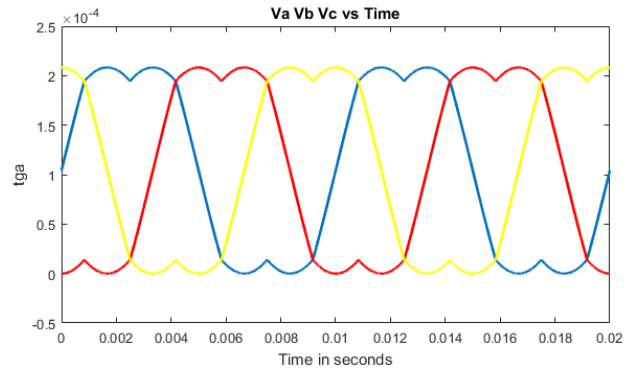


Figure-8. Duty ratio profile with standard SVPWM.

The control of the output voltage is carried out by varying the modulation index in amplitude: $m_a = \frac{v_+}{v_{tri}}$, that is, maintaining the amplitude of the fixed triangular wave, we can vary the pulse width by varying the positive and negative reference voltage [27], [28]. The frequency of the triangular signal imposes the fundamental frequency of the output voltage. In Figure-3, we can observe the v_{tri} signal of the three-phase inverter system.

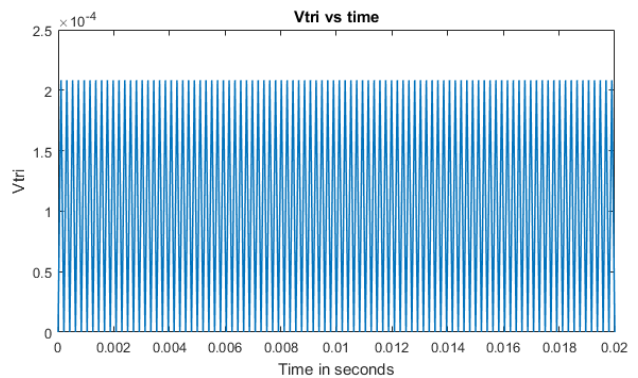


Figure-9. Vtri signal as a function of time.

As shown in Figure-10, the modulating signal of the phase is a composite sinusoidal signal, the result of the sum of two sinusoidal signals. In Figure-10) it can be noted that in the ranges where the fundamental signal [29], [30].

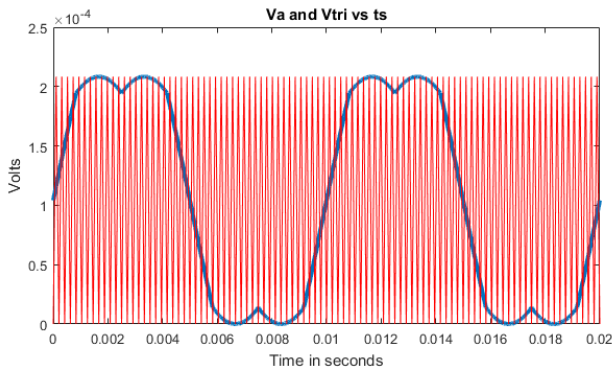


Figure-10. Vtri signal as a function of time.

CONCLUSIONS

This article presented an analysis of the main variations of the Hybrid Control techniques of the Space Vector modulation (SVM), applied to three phase inverters within the scheme of electrical drives for AC motors.

One of the main obstacles in the theoretical study of optimal hybrid control of matrix control is the time used in the calculation that takes the simulation using the Hybrid System toolbox. This restriction was overcome by the mathematical model that is similar to the operation of the power converter stage of the matrix converter.

This will allow some future research in this regard to be much simpler and can progress much more. In order to analyse the correct operation of the optimal hybrid control of the three-phase inverter, it was examined using a mathematical model with induction motor load for a voltage transfer ratio of 0.85.

Therefore, we analyze that there is a certain reward that exists during the use of SVM for inverters of adjustable speed transmission operations using the optimum hybrid control strategy. For the above, we have to choose carefully as to which of the two techniques to use weighing the pros and cons of each method.

REFERENCES

- [1] Celanovic N. & Boroyevich D. 2001. A fast space-vector modulation algorithm for multilevel three-phase converters. *IEEE Transactions on industry applications*. 37(2): 637-641.
- [2] Ruthber Rodriguez Serrezuela, Miguel Ángel Tovar Cardozo, Denicce Licht Ardila and Carlos Andrés Cuellar Perdomo. 2018. A Consistent Methodology for the Development of Inverse and Direct Kinematics of Robust Industrial Robots. *Journal of Engineering and Applied Sciences*, ISSN 819-6608. 13(1): 293-301.
- [3] Zhou K. & Wang D. 2002. Relationship between space-vector modulation and three-phase carrier-based PWM: a comprehensive analysis [three-phase inverters]. *IEEE transactions on industrial electronics*. 49(1): 186-196.
- [4] Serrezuela R. R., Chavarro A. F., Cardozo M. A., Caicedo A. G. R. & Cabrera C. A. 2017. Audio signals processing with digital filters implementation using MyDSP. *Journal of engineering and applied sciences*. 12, 1.
- [5] Narimani M., Yaramasu V., Wu B. & Zargari N. R. 2014, August. A new simplified approach for capacitor voltage balancing of flying capacitor multilevel converters using space vector modulation. In *Power Electronics and Applications (EPE'14-ECCE Europe)*, 2014 16th European Conference on (pp. 1-9). IEEE.
- [6] Montiel J. J. G., Serrezuela R. R. & Aranda E. A. 2017. Applied mathematics and demonstrations to the theory of optimal filters. *Global Journal of Pure and Applied Mathematics*. 13(2): 475-492.
- [7] Deng Y., Teo K. H., Duan C., Habetler T. G. & Harley R. G. 2014. A fast and generalized space vector modulation scheme for multilevel inverters. *IEEE Transactions on Power Electronics*. 29(10): 5204-5217.
- [8] Serrezuela R. R., Cardozo M. A. T. & Chavarro A. F. C. 2017. Design and implementation of a PID fuzzy control for the speed of a DC motor. *Journal of engineering and applied sciences*. 12(8): 2655-2660.
- [9] Zhang Y. & Qu C. 2015. Direct power control of a pulse width modulation rectifier using space vector modulation under unbalanced grid voltages. *IEEE Transactions on Power Electronics*. 30(10): 5892-5901.
- [10] Serrezuela R. R., Chavarro A. F. C., Cardozo M. A. T., Toquica A. L. & Martinez L. F. O. 2017. Kinematic modelling of a robotic arm manipulator using Matlab. *Journal of engineering and applied sciences*. 12(7): 2037-2045.
- [11] Song W., Ma J., Zhou L. & Feng X. 2016. Deadbeat predictive power control of single-phase three-level neutral-point-clamped converters using space-vector modulation for electric railway traction. *IEEE Transactions on power electronics*. 31(1): 721-732.
- [12] J. B. Ramirez Zarta & R. R. Serrezuela. 2017. Solution of System of Differential Equations Deformed with K-Exponential Matrix, In Taekyun



- Kim (Editor), *Advanced Mathematics Theory and Applications*, (pp. 189-204), India, Research India Publications, ISBN: 978-93-84443-20-7.
- [13] Jiao Y., Lee F. C. & Lu S. 2014. Space vector modulation for three-level NPC converter with neutral point voltage balance and switching loss reduction. *IEEE Transactions on Power Electronics*. 29(10): 5579-5591.
- [14] Azhmyakov V., Serrezuela R. R. & Trujillo L. G. 2014, October. Approximations based optimal control design for a class of switched dynamic systems. In *Industrial Electronics Society, IECON 2014-40th Annual Conference of the IEEE* (pp. 90-95). IEEE
- [15] Hu C., Yu X., Holmes D. G., Shen W., Wang Q., Luo F. & Liu N. 2017. An improved virtual space vector modulation scheme for three-level active neutral-point-clamped inverter. *IEEE Transactions on Power Electronics*. 32(10): 7419-7434.
- [16] Serrezuela R. R., Villar O. F., Zarta J. R. & Cuenca Y. H. 2016. The K-Exponential Matrix to solve systems of differential equations deformed. *Global Journal of Pure and Applied Mathematics*. 12(3): 1921-1945.
- [17] Deng Y., Wang Y., Teo K. H. & Harley R. G. 2016. A simplified space vector modulation scheme for multilevel converters. *IEEE Transactions on Power electronics*. 31(3): 1873-1886.
- [18] Rodríguez Serrezuela R. & Carvajal Pinilla L. A. 2015. Ecological determinants of forest to the abundance of *Lutzomyia longiflora* in Tello, Colombia. *International Journal of Ecology*.
- [19] Rojas F., Kennel R., Cardenas R., Repenning R., Clare J. C. & Diaz M. 2017. A new space-vector-modulation algorithm for a three-level four-leg npc inverter. *IEEE Transactions on Energy Conversion*. 32(1): 23-35.
- [20] Serrezuela R. R., Sánchez N. C., Zarta J. B. R., Ardila D. L. & Salazar A. L. P. 2017. Case Study of Energy Management Model in the Threshing System for the Production of White Rice. *International Journal of Applied Engineering Research*. 12(19): 8245-8251.
- [21] Jacob B. & Baiju M. R. 2015. A new space vector modulation scheme for multilevel inverters which directly vector quantize the reference space vector. *IEEE Transactions on Industrial Electronics*. 62(1): 88-95.
- [22] Pinilla L. A. C., Serrezuela R. R., David J., Díaz S., Martínez M. F. & Benavides L. C. L. 2017. Natural Reserves of Civil Society as Strategic Ecosystems: Case Study Meremberg. *International Journal of Applied Environmental Sciences*. 12(6): 1203-1213.
- [23] Sebaaly F., Vahedi H., Kanaan H. Y., Moubayed N. & Al-Haddad K. 2016. Design and implementation of space vector modulation-based sliding mode control for grid-connected 3L-NPC inverter. *IEEE Transactions on Industrial Electronics*. 63(12): 7854-7863.
- [24] Benavides L. C. L., Pinilla L. A. C., Serrezuela R. R. & Serrezuela W. F. R. 2018. Extraction in Laboratory of Heavy Metals through Rhizofiltration using the Plant *Zea Mays* (maize). *International Journal of Applied Environmental Sciences*. 13(1): 9-26.
- [25] Hasan M., Mekhilef S. & Ahmed M. 2014. Three-phase hybrid multilevel inverter with less power electronic components using space vector modulation. *IET Power Electronics*. 7(5): 1256-1265.
- [26] E. García Perdomo, M. A. Tovar Cardozo, C. A. Cuellar Perdomo and R. R. Serrezuela. 2017. A Review of the User Based Web Design: Usability and Information Architecture. *International Journal of Applied Engineering Research*. 12(21): 11685-11690.
- [27] Guo X. 2017. Three-phase CH7 inverter with a new space vector modulation to reduce leakage current for transformerless photovoltaic systems. *IEEE Journal of Emerging and Selected Topics in Power Electronics*. 5(2): 708-712.
- [28] Sánchez N. C., Serrezuela R. R., Ramos A. M. N. & Trujillo J. L. A. 2017. Real Process Characteristic Capacity Weight in the Product 500 Grams in a Rice Mill. *International Journal of Applied Engineering Research*. 12(21): 11588-11597.
- [29] Ahmed S. M., Abu-Rub H. & Salam Z. 2015. Common-Mode Voltage Elimination in a Three-to-Five-Phase Dual Matrix Converter Feeding a Five-Phase Open-End Drive Using Space-Vector Modulation Technique. *IEEE Trans. Industrial Electronics*. 62(10): 6051-6063.
- [30] Serrezuela R. R., Cardozo M. Á. T., Ardila D. L. & Perdomo C. A. C. 2017. Design of a gas sensor based on the concept of digital interconnection IoT for the emergency broadcast system. *Journal of Engineering and Applied Sciences*. 12(22): 6352-6356.



- [31] Zhang M., Atkinson D. J., Ji B., Armstrong M. & Ma M. 2014. A near-state three-dimensional space vector modulation for a three-phase four-leg voltage source inverter. *IEEE Transactions on Power Electronics*. 29(11): 5715-5726.
- [32] Aroca Trujillo J. L., Pérez-Ruiz A. & Rodriguez Serrezuela R. 2017. Generation and Control of Basic Geometric Trajectories for a Robot Manipulator Using CompactRIO®. *Journal of Robotics*, 2017.
- [33] Aroca Trujillo J. L., Rodríguez Serrezuela R., Ramírez Zarta J. B. and Navarrete Ramos A. M. 2018. Direct and Inverse Kinematics of a Manipulator Robot of Five Degrees of Freedom Implemented in Embedded System - CompactRIO, In B. S. Ajaykumar and D. Sarkar, *Advanced Engineering Research and Applications* (pp. 405-419), Nueva Deli, India, Research India Publication.
- [34] Muñoz Calderón Y., Marín Zambrano A. M. and Rodriguez Serrezuela R. 2018. Didactic Mathematical Developments Applied to the Learning of Classic Passive Filters, In B. S. Ajaykumar and D. Sarkar, *Advanced Engineering Research and Applications* (pp. 420-438), Nueva Deli, India, Research India Publication.
- [35] Navarrete Ramos A. M., Aroca Trujillo J. L., Rodríguez Serrezuela R. and Ramírez Zarta J. B. 2018. A Review of the Hotel Sector in the City of Neiva and the Improvement of its Competitiveness through Quality Management Systems, In B. S. Ajaykumar and D. Sarkar, *Advanced Engineering Research and Applications* (pp. 439-452), Nueva Deli, India, Research India Publication.